

vestibular labyrinth (12). This mutant gene is also located on chromosome 2. A chromosome 11 mutant (*teetering*) that also resembles the diver mutant is defective in swimming ability and does not have neuropathological defects visible by light microscopy (13). It differs, however, from diver translocation in that the homozygotes survive as long as a month after birth and have markedly reduced numbers of neurons throughout the central nervous system.

The neurological symptoms are clearly associated with the reciprocal exchange between chromosomes 2 and 14. As far as is known, this is the only neurological mutant in the mouse that resulted from a reciprocal nonhomologous chromosome exchange; all others are either recessive or dominant gene mutations. The translocation marks the genetic location of the defect and provides an avenue for future investigations. The findings also raise the question whether certain human genetic disorders that have been assumed to be the result of single gene mutations may instead be associated with chromosomal rearrangements.

It has been generally assumed that bal-

anced reciprocal translocations do not involve loss or gain in chromosomal components. For example, high-resolution karyotype analysis (at the level of light microscopy) of 13 human carriers of balanced translocations did not demonstrate any net loss or gain of chromosomal material (14). However, an increasing number of clear associations between balanced exchange and deleterious effects suggest that either the breakpoint may be located inside a structural gene or that it may affect the activity of genes in the immediate vicinity. In a female patient with Duchenne muscular dystrophy resulting from a translocation involving one X chromosome, the breakpoint is located close to the Duchenne muscular dystrophy gene (15). Little is known about the molecular mechanism involved in the formation of mutagen-induced nonhomologous chromosomal exchange. The diver translocation mutant may prove useful not only in neurobiology, but also in understanding the molecular nature of chemically induced chromosome exchange and the way in which deleterious effects of the exchange are expressed.

#### REFERENCES AND NOTES

1. S. J. Funderburk, M. A. Spence, R. S. Sparkes, *Am. J. Hum. Genet.* **29**, 136 (1977).
2. V. Ventruto *et al.*, *ibid.* **16**, 589 (1983).
3. N. Tommerup and F. Nielsen, *ibid.* **16**, 313 (1983).
4. C. Verellen-Dumoulin *et al.*, *Hum. Genet.* **67**, 115 (1984).
5. W. M. Generoso, M. Krishna, K. T. Cain, C. W. Sheu, *Mutat. Res.* **81**, 177 (1981).
6. W. M. Generoso, K. T. Cain, M. Krishna, C. W. Sheu, R. M. Gryder, *ibid.* **73**, 133 (1980).
7. W. M. Generoso *et al.*, *Genetics* **100**, 633 (1982).
8. W. M. Generoso, K. T. Cain, N. L. A. Cacheiro, C. V. Cornett, *Mutat. Res.* **126**, 177 (1984).
9. P. Selby, paper presented at the 14th International Congress of Genetics, Moscow, 1978.
10. E. P. Evans, G. Breckon, C. E. Ford, *Cytogenetics* **3**, 289 (1964).
11. N. L. A. Cacheiro and L. B. Russell, *Genet. Res.* **25**, 193 (1975).
12. D. Lim, *Birth Defects Orig. Art. Ser.* **16**, III (1980).
13. H. Meier, *Arch. Neurol.* **16**, 59 (1967).
14. S. C. Raimondi, F. W. Luthardt, R. L. Summitt, P. R. Martens, *Hum. Genet.* **63**, 310 (1983).
15. R. G. Worton, C. Duff, J. E. Sylvester, R. D. Schmittel, H. F. Willard, *Science* **224**, 1447 (1984).
16. M. Nesbitt and U. Francke, *Chromosoma* **41**, 145 (1973).
17. We thank M. Henderson and M. Hardesty for preparation of the manuscript. Sponsored by the Office of Health and Environmental Research, U.S. Department of Energy, under contract DE-AC05-84OR21400 with the Martin Marietta Energy Systems, Inc.

24 June 1985; accepted 25 October 1985

## A Blood Vessel Model Constructed from Collagen and Cultured Vascular Cells

CRISPIN B. WEINBERG AND EUGENE BELL

**A model of a blood vessel was constructed in vitro. Its multilayered structure resembled that of an artery and it withstood physiological pressures. Electron microscopy showed that the endothelial cells lining the lumen and the smooth muscle cells in the wall were healthy and well differentiated. The lining of endothelial cells functioned physically, as a permeability barrier, and biosynthetically, producing von Willebrand's factor and prostacyclin. The strength of the model depended on its multiple layers of collagen integrated with a Dacron mesh.**

**A** MODEL OF A BLOOD VESSEL THAT reproduces in vitro many of the physical and biological characteristics of a mammalian artery would be useful for the study of vascular cell biology, physiology, and pathology. Such a model might also be used as a living vascular prosthesis to replace or bypass small caliber arteries (<6 mm inside diameter) for which synthetic and processed biological grafts have not been entirely successful (1). Vascular cells have been extensively studied in tissue culture (2). Some aspects of the vascular wall have been replicated in vitro when endothelial cells were grown, not on plastic substrates, but in more physiological environments—on extracellular matrix materials, on layers of smooth muscle cells, under flow, or

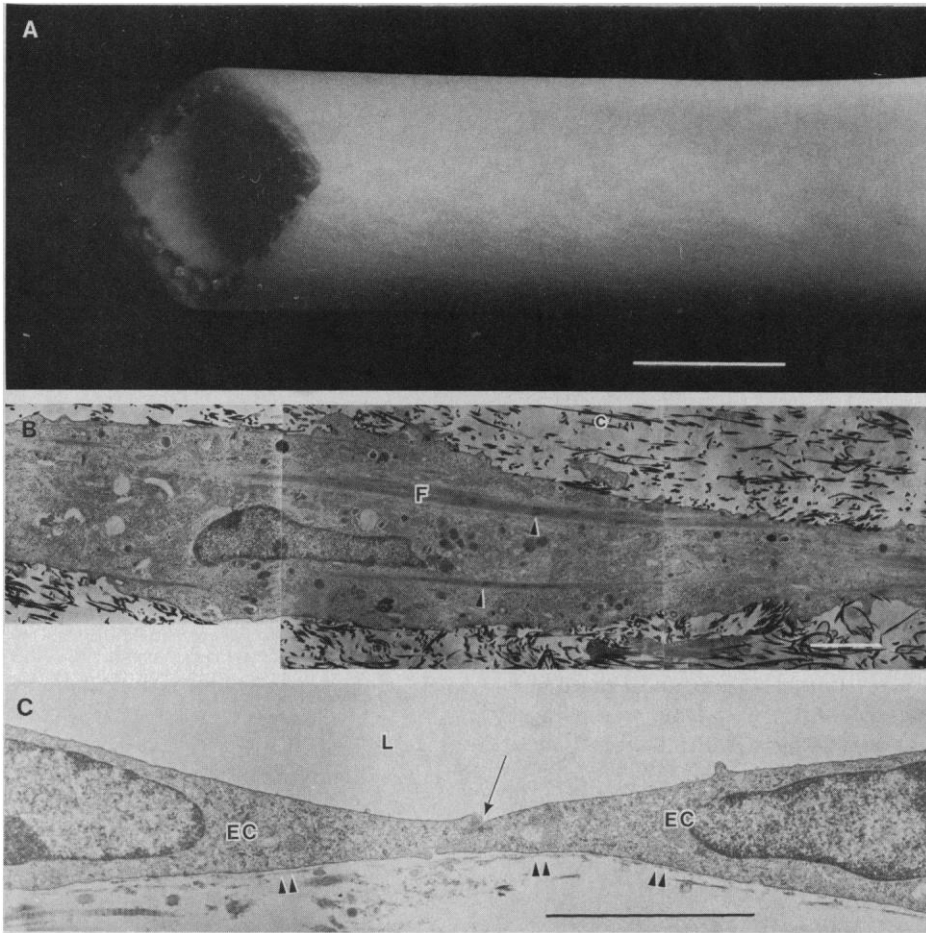
in a mock circulatory loop (3). Combining these approaches might result in the ideal blood vessel model, a multilayered tube capable of withstanding physiological pressures, allowing access to luminal and abluminal fluid compartments, and able to be incorporated into a mock circulatory loop. The layers corresponding to the intima, media, and adventitia would consist of a confluent monolayer of endothelial cells lining the lumen, a middle layer with a high density of smooth muscle cells and matrix materials, and an outer layer with adventitial fibroblasts and matrix materials.

We have developed a blood vessel model that meets these criteria. The construction of the model is based on the observations that fibroblasts can contract a hydrated collagen

gel by a factor of 10 to 20 to produce a tough tissue-like lattice and that such a lattice is a suitable substrate for epithelial cells (4). In this report, we describe the construction of our model, demonstrate that the layer of endothelial cells functions much like the endothelium of a normal blood vessel, and examine the effects of various parameters on the strength of the model. A preliminary report of this model has been presented (5).

Bovine aortic endothelial cells, smooth muscle cells, and adventitial fibroblasts were isolated and cultured by standard methods (2). The middle layer of the blood vessel model, corresponding to the media of an artery, was prepared by casting culture medium, collagen, and smooth muscle cells together in an annular mold (4, 6). The mixture jelled after a few minutes at 37°C and contracted within a few days to produce a tubular lattice around the central mandrel. After 1 week, an open Dacron mesh sleeve was slipped over the lattice to provide additional mechanical support. The outer layer, corresponding to the adventitia, was cast around the first lattice with adventitial fibroblasts rather than smooth muscle cells. Two weeks later, when the outer layer was fully

Department of Biology, Massachusetts Institute of Technology, Cambridge 02139.



contracted, the tube was carefully slipped off the mandrel with jeweler's forceps and either used for mechanical testing or lined with endothelial cells. For the latter, the model was cannulated, a suspension of endothelial cells was injected into the lumen, and the vessel was rotated around the longitudinal axis at 1 rev/min for 1 week to distribute endothelial cells uniformly on the luminal surface.

The model grossly resembled a muscular artery, except for the Dacron mesh (Fig. 1A). Electron microscopy showed that the smooth muscle cells are well-differentiated bipolar cells containing bundles of filaments with dense bodies (Fig. 1B). They frequently appeared to be secreting collagen into the

Fig. 1. Structure of the blood vessel model. (A) Whole mount of a blood vessel model cut obliquely to reveal the lumen. Scale bar, 5 mm. (B) Electron micrograph of the wall of the blood vessel model showing a smooth muscle cell and collagen fibers (c). Bundles of filaments (F) with dense bodies (arrowheads) characterize the smooth muscle cell. (C) Electron micrograph showing parts of two endothelial cells (EC) lining the lumen (L) with an intercellular junction (arrow), and patches of basement membrane (arrowheads). (B) and (C) were fixed in buffered glutaraldehyde, postfixed with osmium, embedded in Spurr's resin, sectioned, and stained with uranyl acetate and lead citrate. Scale bars in (B) and (C), 2  $\mu$ m.

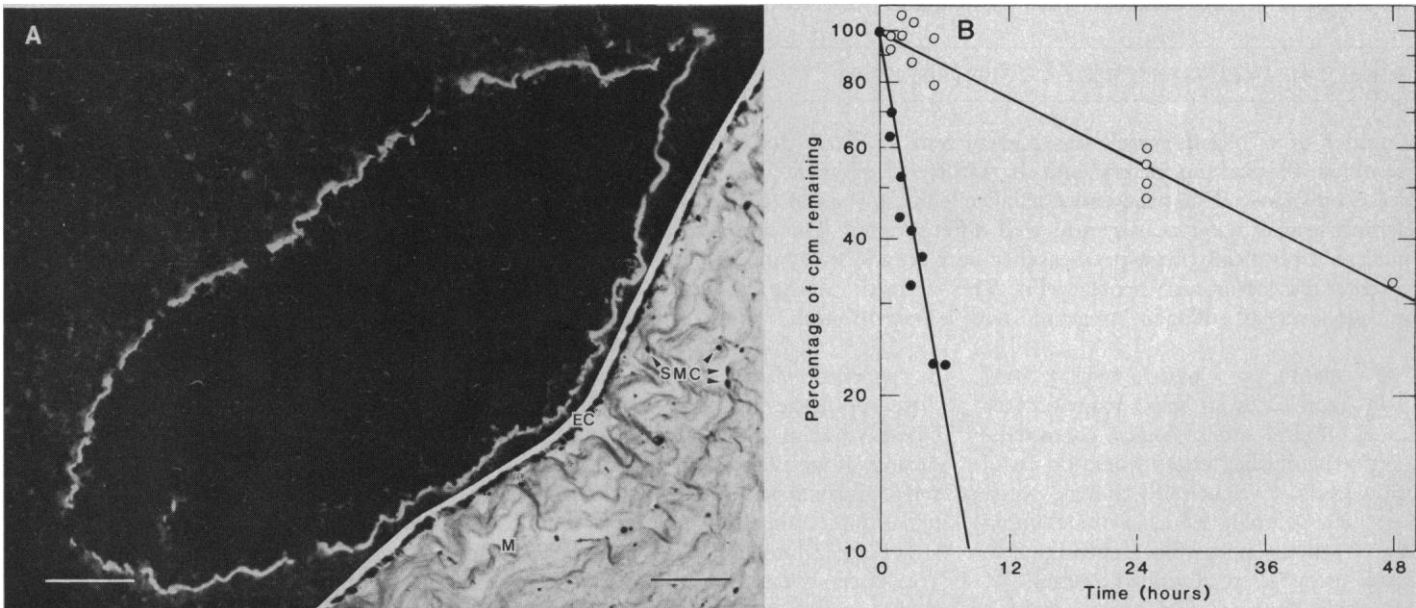
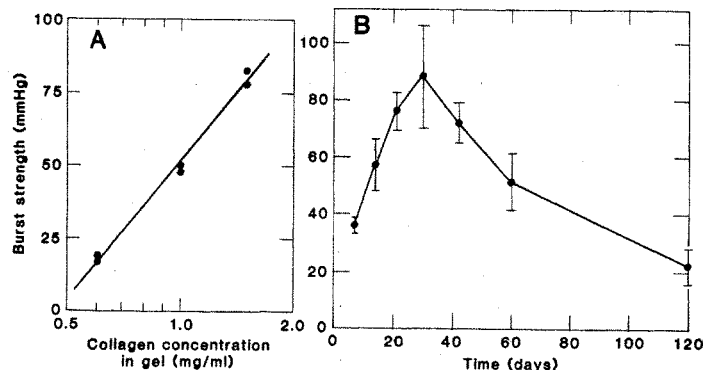


Fig. 2. Function of the endothelial lining. (A) Montage showing localization of von Willebrand factor (factor VIII-related antigen) by indirect immunofluorescence. A cryostat section of a 2-mm model was incubated with a rabbit antiserum to von Willebrand factor (Calbiochem-Behring) and then with fluorescein-conjugated goat antibody to rabbit immunoglobulin G (Cappel Laboratories). Control models prepared without an endothelial lining did not show fluorescence on the luminal surface. Inset: Light micrograph of the wall of a model showing the monolayer of endothelial cells (EC), smooth muscle cells (SMC), and the collagen matrix (M). A 6- $\mu$ m paraffin cross section was stained with Milligan's trichrome so that cell bodies are darkly stained and collagen fibers are distinct. Scale bars, 250  $\mu$ m

(A); 50  $\mu$ m (inset). (B) Diffusion of albumin across the vessel model wall. Models were cannulated, placed in a bath of culture medium, and perfused with  $^{14}$ C-labeled bovine serum albumin (New England Nuclear), 0.3  $\mu$ Ci/ml, in culture medium. Duplicate 10- $\mu$ l aliquots were removed from the lumen at intervals, dried on filter paper, and counted in a liquid scintillation counter. Values shown are averages of duplicate aliquots from individual models (open circles,  $n = 4$ ) and from control models prepared without an endothelial lining (closed circles,  $n = 2$ ). Curves were fitted by linear regression, giving half-times of  $28.1 \pm 1.5$  hours and  $2.8 \pm 0.3$  hours, respectively.

Fig. 3. Burst strength of the blood vessel model. (A) Burst strength as a function of collagen concentration in the wall. Models were prepared with collagen solutions ranging from 2 to 5 mg/ml to give the initial concentrations shown. More concentrated collagen solutions were too viscous to be mixed with the remaining lattice components. Models were tested 2 weeks after the second layer was cast. Values shown are individual determinations and the line was drawn by linear regression. (B) Models were tested at various times after the second layer was cast. Values shown are means  $\pm$  SEM ( $n = 4$  to 6). Burst strengths were measured by cannulating the models in a buffered saline bath and filling them at 5 ml/min with saline containing a blue dye for contrast. Pressure was monitored with a pressure transducer connected to a chart recorder. Burst strength was defined as the pressure at which the model either ruptured or developed a visible leak.



extracellular space, thus contributing to the matrix (7). The endothelial cells formed a monolayer of flattened cells with intercellular junctions, numerous vesicles, occasional Weibel-Palade bodies, and patches of basement membrane by 1 week (Fig. 1C). Scanning electron microscopy showed that virtually the entire luminal surface was covered by endothelial cells. Histological measurements demonstrated that endothelial cells covered at least  $92.1 \pm 2.5$  percent [mean  $\pm$  standard error of the mean (SEM),  $n = 3$ ] of the surface. This value is a lower limit for coverage since some of the endothelial cells were lost during processing for histology. The distribution of cells in the inner layers of the model was examined by light microscopy (Fig. 2A, inset).

The endothelial lining of the blood vessel model functioned like a normal endothelium in several respects. It produced von Willebrand factor (Fig. 2A), a widely used marker for vascular endothelium (8), and it formed a permeability barrier for large molecules such as albumin (Fig. 2B). Endothelial cells release prostacyclin, which is a potent inhibitor of platelet aggregation and is believed to prevent thrombosis in vivo (9). Prostacyclin production was measured by radioimmunoassay of 6-keto-prostaglandin  $F_{1\alpha}$ , the stable metabolite of prostacyclin, after the model was stimulated with  $20 \mu M$  arachidonic acid for 2 minutes (10). The endothelialized model released prostacyclin at a rate of  $3.4 \pm 1.2 \text{ ng} \cdot \text{cm}^{-2} \cdot \text{min}^{-1}$ , whereas the model without an endothelial lining released very little prostacyclin ( $0.4 \text{ ng} \cdot \text{cm}^{-2} \cdot \text{min}^{-1}$ ). The rate for the endothelialized model is comparable to rates calculated from published data (10) for endothelial cells grown on plastic and for normal rabbit aorta ( $4.8 \pm 0.9$  and  $8.4 \pm 2.2 \text{ ng} \cdot \text{cm}^{-2} \cdot \text{min}^{-1}$ , respectively).

The ability of the blood vessel model to withstand intraluminal pressure depended on several factors including the mesh, collagen concentration, initial cell density, and time elapsed after casting. The role of these

factors was assessed by measuring the burst strengths of models made by varying these parameters from the standard protocol (6). A model made without the mesh was so highly distensible that it dilated and ruptured with a longitudinal tear (1 to 2 cm long) at very low pressures ( $<10$  mmHg). The standard model made with one mesh, while still quite compliant, had a burst strength of 40 to 70 mmHg and typically failed by delaminating and tearing. A model constructed with three layers of collagen lattice alternating with two meshes had a burst strength of 120 to 180 mmHg and usually failed by developing a pinhole leak. The burst strength of the model was proportional to the logarithm of the collagen concentration (Fig. 3A). Over a wide range of initial cell densities ( $2 \times 10^4$  to  $2 \times 10^5$  cells per milliliter in the casting mixture) there was no significant variation in burst strength. At much lower cell densities the lattice contracted poorly (4) and was too flimsy to be tested. At much higher cell densities the lattice contracted so tightly around the mandrel that it could withstand only slight dilation and failed at 10 to 30 mmHg. A blood vessel model attained its maximal burst strength 3 to 6 weeks after casting (Fig. 3B). The increase in strength with time is probably due to cross-linking of the collagen. The decrease in strength after long times may be caused by collagenase secreted by the smooth muscle cells and fibroblasts in the lattices (11). To maximize the burst strength, we optimized the above parameters (12) and produced models with a burst strength of  $323 \pm 31$  mmHg (mean  $\pm$  SEM,  $n = 5$ ).

Thus, our model meets many of the physiological and physical criteria for a blood vessel model; however, there are substantial differences between the model and normal arteries in addition to the requirement for the Dacron mesh. A major difference is that we are unable to include elastin, the principal arterial connective tissue protein besides collagen, in the matrix mixture, although

small amounts of elastin may be synthesized by the smooth muscle cells after long periods in culture. A significant structural difference is that the smooth muscle cells and collagen fibers have a largely longitudinal orientation, because the contraction of the lattice layers around the mandrel is primarily radial rather than in the alternating left- and right-handed spirals of blood vessels. This may explain why a model that was not supported by a mesh failed by splitting lengthwise. A third difference is that the densities of smooth muscle cells and collagen in the model are one-eighth to one-fourth those in normal blood vessels.

We have demonstrated that our model reproduces in vitro many of the characteristics of a mammalian muscular artery. The model is appropriate for studying the interactions of vascular cells with each other, with components of the extracellular matrix, and with rheological forces, and for studying transport across the endothelium. It may be possible to use the model to replicate in vitro aspects of atherogenesis, tumor invasion, and other pathological processes. If the model is sufficiently durable after implantation in animals, and the immunological barrier to allografts can be overcome, as has been possible for some cell types (13), then models constructed with human cells might serve as living vascular prostheses for small-caliber arteries. Our blood vessel model is attractive for this application since it is lined with a functional endothelium and since it could heal at an anastomosis to become truly integrated with the host's vasculature.

#### REFERENCES AND NOTES

1. J. C. Stanley, Ed., *Biologic and Synthetic Vascular Prostheses* (Grune & Stratton, New York, 1982).
2. J. Chamley-Campbell, G. Campbell, R. Ross, *Physiol. Rev.* **59**, 1 (1979); M. A. Gimbrone, *Prog. Hemost. Thromb.* **3**, 1 (1976); E. A. Jaffe, R. L. Nachman, C. G. Becker, R. C. Minick, *J. Clin. Invest.* **52**, 2745 (1973); R. Ross, *J. Cell Biol.* **50**, 172 (1971); D. Shepro and P. A. D'Amore, *Adv. Microcirc.* **9**, 161 (1980).
3. E. I. Chazov *et al.*, *Proc. Natl. Acad. Sci. U.S.A.* **78**, 3603 (1981); C. F. Dewey, S. R. Bussolari, M. A. Gimbrone, P. F. Davies, *J. Biomech. Eng.* **103**, 177 (1981); S. G. Eskin, L. T. Navarro, W. O'Bannon,

M. E. Debakey, *Artif. Org.* 7, 31 (1983); D. Gospodarowicz, I. Vlodavsky, N. Savion, *J. Supramol. Struct.* 13, 339 (1980); P. A. Jones, *Proc. Natl. Acad. Sci. U.S.A.* 76, 1882 (1979).

4. E. Bell, B. Ivarsson, C. Merrill, *Proc. Natl. Acad. Sci. U.S.A.* 76, 1274 (1979); E. Bell, H. P. Erlich, D. J. Buttle, T. Nakatsuji, *Science* 211, 1052 (1981); C. B. Weinberg and E. Bell, *J. Cell. Physiol.* 122, 410 (1985).

5. C. B. Weinberg and E. Bell, *J. Cell Biol.* 99, 66A (1984).

6. For most experiments, the mold was a 25-mm test tube with a 6-mm polished glass mandrel, although models have been made with internal diameters from 2 mm to 1 cm. The standard model, 7.5 cm long, was made with a mixture of 13.8 ml of 1.76× McCoy's 5A medium supplemented with antibiotics and 2.7 ml of fetal bovine serum (Flow Laboratories or Gibco Laboratories), 1.5 ml of 0.1N NaOH, 9.0 ml of porcine skin collagen (produced by Pentapharm A.G. and kindly provided by Centrechem) or

rat tail tendon collagen dissolved at 3.2 to 3.4 mg/ml in 0.1 percent acetic acid, and 3.0 ml of culture medium containing  $5 \times 10^5$  smooth muscle cells per milliliter.

7. B. Nussgens, C. Merrill, C. Lapierre, E. Bell, *Collagen Rel. Res.* 4, 351 (1984); D. E. Birk and R. L. Trellstad, *J. Cell Biol.* 99, 2024 (1984).

8. L. W. Hoyer, R. P. de los Santos, J. R. Hoyer, *J. Clin. Invest.* 52, 2737 (1973); E. A. Jaffe, L. W. Hoyer, R. L. Nachman, *J. Clin. Invest.* 52, 2757 (1973).

9. S. Bunting, R. Grygleski, S. Moncada, J. R. Vane, *Prostaglandins* 12, 897 (1976); B. B. Weksler, A. J. Marcus, E. A. Jaffe, *Proc. Natl. Acad. Sci. U.S.A.* 74, 3922 (1977).

10. A. Eldor, D. J. Falcone, D. P. Hajjar, C. R. Minick, B. B. Weksler, *J. Clin. Invest.* 67, 735 (1981); A. Eldor et al., *J. Cell Physiol.* 114, 179 (1983).

11. U. Delvos, C. Gajdusek, H. Sage, L. A. Harker, S. M. Schwartz, *Lab. Invest.* 46, 61 (1982).

12. The optimized models had three layers of collagen

and cells alternating with two meshes ( $1 \times 10^5$  cells and 1.5 mg of collagen per milliliter were used in the casting mixture) and had been aged for 1 month in vitro.

13. D. Faustman, V. Hauptfeld, P. Lacy, J. Davie, *Proc. Natl. Acad. Sci. U.S.A.* 78, 5156 (1981); K. J. Lafferty, A. Bootes, G. Part, D. W. Talmage, *Transplantation* 22, 138 (1976); H. Lau, K. Reemsta, M. A. Hardy, *Science* 221, 754 (1983); S. E. Sher, B. E. Hull, S. Rosen, D. Church, L. Friedman, E. Bell, *Transplantation* 36, 552 (1983).

14. We thank L. D. Honaryar, C. Merrill, and H. Youssoufian for culturing cells, and H. Moore for histological assistance. We are grateful to H. B. Haines for performing the electron microscopy, which was carried out with the assistance of E. Hartwig of the Department of Biology Electron Microscope Facility, Massachusetts Institute of Technology

28 June 1985; accepted 23 October 1985

## Sevenless: A Cell-Specific Homeotic Mutation of the *Drosophila* Eye

ANDREW TOMLINSON AND DONALD F. READY

Each ommatidium in the compound eye of the *Drosophila* mutant *sevenless* lacks photoreceptor number seven (R7) from the normal ommatidial complement of eight photoreceptors. A comparison of mutant and normal development reveals that this deficit is caused by the cell-specific transformation of the cell normally fated to produce R7 into a lens-secreting accessory cell, a cone cell.

**D**URING DEVELOPMENT, CELLS SELECT pathways of specialization that lead to the differentiation of particular cell types. Disturbances of this selection process can lead to the substitution of a normal pattern element with one appropriate

ate to another location; the term homeosis was introduced to describe this condition (1). For example, in *Drosophila* the homeotic mutation *bithorax* directs cells normally destined to differentiate metathoracic structures to produce their mesothoracic counterparts (2). We studied compound eye development in the *Drosophila* mutant *sevenless* (3), in which each ommatidium lacks photoreceptor number seven (R7) from the normal ommatidial complement of eight photoreceptors (4, 5). In the developing mutant ommatidium, a cell occupies the site normally taken by the prospective R7 cell. Instead of becoming a photoreceptor, however, the cell differentiates into a lens-secreting cone cell. Thus *sevenless* is a cell-specific homeotic mutation, precisely switching the developmental fate of one cell to that of another.

The developing compound eye of *Drosophila* is well suited to an examination of pathway selection at the level of individual cells. Each of the approximately 750 ommatidia that comprise the compound eye is a stereotyped cellular assembly in which every cell can be identified by its unique position. This architectural stereotypy applies also to the developing ommatidia, permitting the fate of a cell to be read from its characteristic position as it joins the assembly (6, 7).

The compound eye grows by the sequential addition of new ommatidial precursors to its anterior margin (8); anterior ommatidia are younger than posterior ones. Since each ommatidial precursor is slightly more developed than its anterior neighbor, a maturational gradient is laid out spatially along the anterior-posterior axis of the epithelium. Electron microscopic reconstruction of a series of precursors lying along the maturational axis thus reveals the smooth progression of stages through which an individual

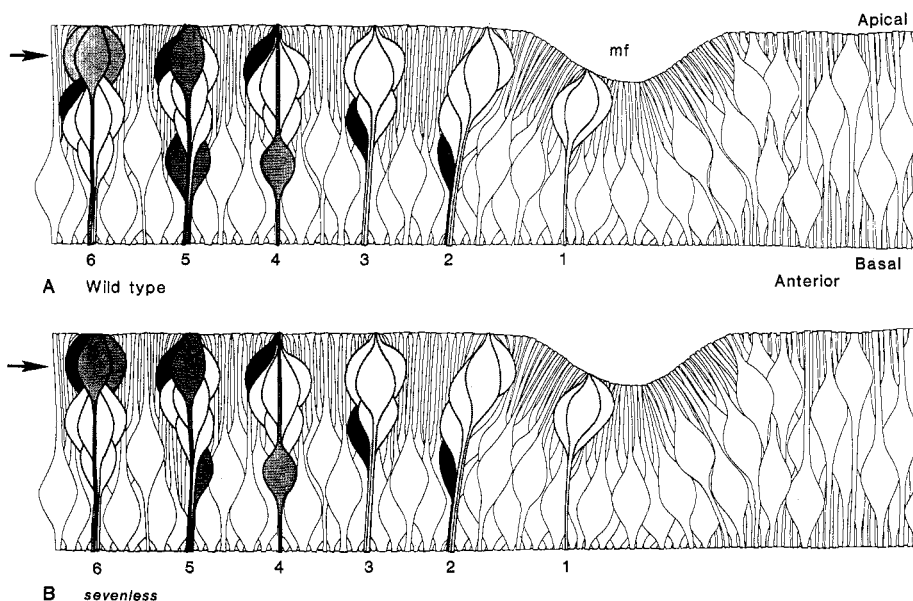


Fig. 1. Schematic side view of ommatidial assembly in wild type (A) and *sevenless* (B) (not all precursor cells shown). All cells (except for dividing cells, not shown) extend from the apical surface to the basement membrane of the epithelium. The nuclei are located in the cell bodies. Photoreceptor R7, black; cone cells, dark gray; photoreceptors R1 to R6 and R8, light gray; all other cells, white; and mf, morphogenetic furrow. Arrows indicate plane of sections shown in Fig. 2. (A) Region 1 comprises a five-cell precluster. In region 2, R1, R6, and R7 rise to join the precursor. Region 3 contains a symmetrical cluster. In region 4, as R7 completes apical migration, two cone cell nuclei rise. In region 5 two more cone cell nuclei rise. In region 6 four cone cell nuclei overlie the photoreceptors. (B) Regions 1, 2, 3, and 4 are as described in (A). In region 5 only a single cone cell nucleus rises. In region 6 the cell in the R7 position remains apical and joins the cone cell unit; only seven photoreceptors sink basally.

Department of Biology, Princeton University, Princeton, NJ 08540.